

Low-temperature negative thermal expansion of the antiperovskite manganese nitride Mn_3CuN codoped with Ge and Si

Rongjin Huang, Laifeng Li, Fangshuo Cai, Xiangdong Xu, and Lihe Qian

Citation: *Applied Physics Letters* **93**, 081902 (2008); doi: 10.1063/1.2970998

View online: <http://dx.doi.org/10.1063/1.2970998>

View Table of Contents: <http://scitation.aip.org/content/aip/journal/apl/93/8?ver=pdfcov>

Published by the *AIP Publishing*

Articles you may be interested in

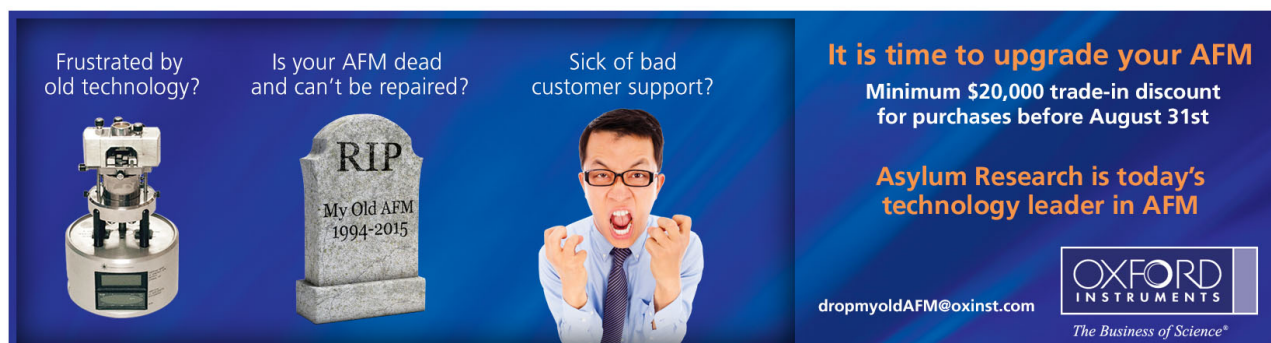
[Effects of nitrogen deficiency on the magnetostructural properties of antiperovskite manganese nitrides](#)
J. Appl. Phys. **111**, 07E314 (2012); 10.1063/1.3672243

[Giant negative thermal expansion in antiperovskite manganese nitrides](#)
J. Appl. Phys. **109**, 07E309 (2011); 10.1063/1.3540604

[Local structure anomaly around Ge dopants in \$\text{Mn}_3\text{Cu}_{0.7}\text{Ge}_{0.3}\text{N}\$ with negative thermal expansion](#)
Appl. Phys. Lett. **94**, 181904 (2009); 10.1063/1.3129169

[Zero thermal expansion in a pure-form antiperovskite manganese nitride](#)
Appl. Phys. Lett. **94**, 131904 (2009); 10.1063/1.3110046

[Giant negative thermal expansion in Ge-doped anti-perovskite manganese nitrides](#)
Appl. Phys. Lett. **87**, 261902 (2005); 10.1063/1.2147726

An advertisement for Oxford Instruments' AFM upgrade program. The background is dark blue. On the left, there is a photo of an old AFM. In the center, a tombstone reads 'RIP My Old AFM 1994-2015'. To the right of the tombstone is a man with glasses, looking frustrated with his hands raised. Text on the left asks 'Frustrated by old technology?', 'Is your AFM dead and can't be repaired?', and 'Sick of bad customer support?'. On the right, it says 'It is time to upgrade your AFM', 'Minimum \$20,000 trade-in discount for purchases before August 31st', and 'Asylum Research is today's technology leader in AFM'. At the bottom right is the Oxford Instruments logo and the tagline 'The Business of Science®'. The email 'dropmyoldAFM@oxinst.com' is at the bottom left of the ad area.

Frustrated by old technology?

Is your AFM dead and can't be repaired?

Sick of bad customer support?

It is time to upgrade your AFM

Minimum \$20,000 trade-in discount for purchases before August 31st

Asylum Research is today's technology leader in AFM

dropmyoldAFM@oxinst.com

OXFORD
INSTRUMENTS
The Business of Science®

Low-temperature negative thermal expansion of the antiperovskite manganese nitride Mn_3CuN codoped with Ge and Si

Rongjin Huang,^{1,2} Laifeng Li,^{1,a)} Fangshuo Cai,^{1,2} Xiangdong Xu,¹ and Lihe Qian³

¹Technical Institute of Physics and Chemistry, Chinese Academy of Sciences, Beijing 100190, China

²Graduate University of Chinese Academy of Sciences, Beijing 100080, China

³Research Institute for Applied Mechanics, Kyushu University, 6-1 Kasuga-koen, Kasuga 816-8580, Japan

(Received 7 July 2008; accepted 18 July 2008; published online 25 August 2008)

We have synthesized antiperovskite manganese nitrides $\text{Mn}_3(\text{Cu}_{0.6}\text{Si}_x\text{Ge}_{0.4-x})\text{N}$, ($x=0-0.2$) and investigated their negative thermal expansion (NTE) in the temperature range of 80–300 K. We found that the transition temperature of NTE moves toward lower temperature region and as well the NTE operation-temperature window (ΔT) becomes broader with increasing Si content. Typically, the giant low-temperature NTE coefficient identified in $\text{Mn}_3(\text{Cu}_{0.6}\text{Si}_{0.15}\text{Ge}_{0.25})\text{N}$ reaches as large as $-16 \times 10^{-6} \text{ K}^{-1}$, and its ΔT reaches as wide as 100 K. The magnetic properties of these compounds were measured and correlated with the broadened NTE operation-temperature window. The present discovery highlights the potential applications of NTE materials in cryogenic engineering. © 2008 American Institute of Physics. [DOI: 10.1063/1.2970998]

As is well known, a very limited number of materials exhibits “abnormal” negative thermal expansion (NTE), i.e., they contract on heating. NTE materials can be mixed with materials showing positive thermal expansion to form composites with a desired overall thermal expansion coefficient. Hence, there may be many potential applications of NTE materials used as, for example, optical fiber reflective grating device, high-precision optical mirrors, printed circuit boards, and teeth fillings.^{1,2} The study of NTE materials has gained considerable impetus. Examples of the most studied NTE materials include several oxide systems such as ZrW_2O_8 (Refs. 3 and 4) and HfW_2O_8 ,⁵ a few invar alloys,^{6,7} and some antiperovskite manganese nitrides.^{8–10} It is noteworthy, however, that most researchers focus their attention on the NTE behavior around or above room temperature, while there are few reports on NTE for low-temperature applications. In fact, low-temperature NTE materials have wide potential applications in microelectromechanical systems in space and superconducting magnets such as low heat leak cryogenic valve, piston/piston sleeve of refrigerator, and carrying construction of superconducting magnet. The purpose of this letter is, thus, to synthesize NTE materials for applications in cryogenic engineering.

We note that one important mechanism for NTE is the magnetovolume effect (MVE). Here, we are intrigued by the large MVE of the antiperovskite manganese nitride Mn_3AN ($A=\text{Zn}$, Ga , etc.).⁸ These compounds do demonstrate large NTE, however, they have not been considered for practical NTE applications due to their sharp, discontinuous change in volume at transition.^{9,10} More recently, Takenaka and co-workers^{9,10} discovered that the discontinuous expansion of the nitride compound Mn_3AN ($A=\text{Cu}$, Zn) on heating changes to continuous expansion after partial substitution of element Ge or Sn for A. The Ge- or Sn-doped Mn_3AN ($A=\text{Cu}$, Zn) were demonstrated to show excellent NTE property around or above room temperature. For example, $\text{Mn}_3(\text{Cu}_{0.53}\text{Ge}_{0.47})\text{N}$ (Ref. 9) show large NTE coefficients of

$\alpha = -16 \times 10^{-6} \text{ K}^{-1}$ at $T=267-342 \text{ K}$ and broad NTE operation-temperature window of $\Delta T=75 \text{ K}$. However, $\text{Mn}_3(\text{Cu}_{1-x}\text{B}_x)\text{N}$ ($B=\text{Ge}$, Sn) still show sharp, discontinuous volume change with very narrow operation-temperature windows at cryogenic temperatures. Consequently, an obvious issue is how to shift the NTE temperature of $\text{Mn}_3(\text{Cu}_{1-x}\text{B}_x)\text{N}$ ($B=\text{Ge}$, Sn) to low-temperature region, while maintaining or broadening the NTE operation-temperature window.

The MVE temperature of Mn_3AN is affected by the “electron concentration” around element A.⁸ We notice that element Si has the same valence electrons as Ge and Sn, but has fewer electron shells. Accordingly, Si is assumed to have chemically similar properties to Ge and Sn, and therefore partial replacement of Si for Ge or Sn may provide a possibility of lowering the NTE temperature in $\text{Mn}_3(\text{Cu}_{1-x}\text{B}_x)\text{N}$ ($B=\text{Ge}$, Sn). In this letter, we examined this possibility and studied the effects of Si doping on thermal expansion properties of the $\text{Mn}_3(\text{Cu}_{0.6}\text{Ge}_{0.4-x}\text{Si}_x)\text{N}$. We found that Si doping indeed lowers the NTE transition temperature and as well broadens the NTE operation-temperature window at cryogenic temperatures.

The polycrystalline samples with general formula $\text{Mn}_3(\text{Cu}_{0.6}\text{Si}_x\text{Ge}_{0.4-x})\text{N}$ ($x=0, 0.05, 0.1, 0.15, 0.2$) were prepared by a solid state reaction method. First, Mn_3N powders were synthesized by flowing purified nitrogen gas into pure Mn powders at 750°C for 60 h. Then, the powders of Cu (99.99 at. %), Si (99.99 at. %), Ge (99.99 at. %), and Mn_3N were mechanical ball milled in a planetary ball mill at a rotating speed of 350 rpm for 24 h. The as-milled powders were preformed under a pressure of 500 MPa at room temperature. The preformed samples were wrapped with tantalum foil and sintered at 850°C under a purified argon atmosphere for 48 h.

The crystal structures were characterized at room temperature by x-ray diffraction (XRD) analysis using Rigaku D/max-RB diffractometer with $\text{Cu K}\alpha$ radiation. The linear thermal expansion data ($\Delta L/L_{(300 \text{ K})}$) was measured using a strain gage over a temperature range of 80–300 K. According to Ref. 9 we used fused silica and its corresponding linear thermal expansion data as the reference.¹¹ Magnetic suscep-

^{a)}Author to whom correspondence should be addressed. Tel.: +86 10 82543699. Electronic mail: lffi@mail.ip.ac.cn.

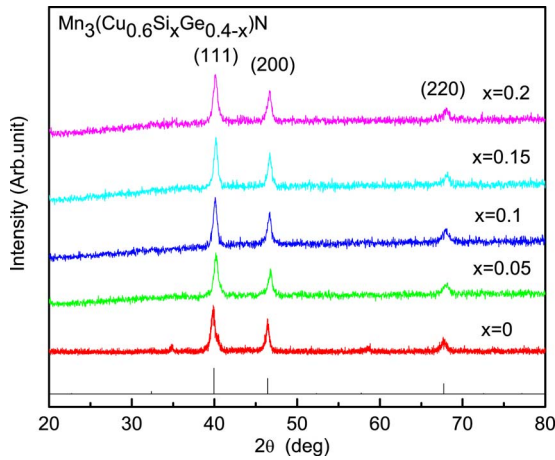


FIG. 1. (Color online) XRD patterns for $\text{Mn}_3(\text{Cu}_{0.6}\text{Si}_x\text{Ge}_{0.4-x})\text{N}$ ($x=0, 0.05, 0.1, 0.15, 0.2$) samples at room temperature.

tibility was measured using a magnetic balance in a field of 1.2 T in the temperature range of 80–300 K.

Figure 1 shows the x-ray patterns of $\text{Mn}_3(\text{Cu}_{0.6}\text{Si}_x\text{Ge}_{0.4-x})\text{N}$ ($x=0, 0.05, 0.1, 0.15, 0.2$) at room temperature. The indices of crystallographic plane (hkl) of reflections are shown. It indicates that these samples have a dominating phase with the Mn_3CuN -type structure (space group, $Pm\bar{3}m$) (Ref. 12). There are no visible diffraction peaks of pure elements and other second phases in the XRD patterns.

The $\Delta L/L_{300\text{ K}}$ obtained for samples $\text{Mn}_3(\text{Cu}_{0.6}\text{Si}_x\text{Ge}_{0.4-x})\text{N}$ ($x=0, 0.05, 0.1, 0.15, 0.2$) are shown in Fig. 2(a). It can be seen that for each sample there exists a temperature region in which the linear thermal expansion increases with decreasing temperature, i.e., NTE occurs. The sample $\text{Mn}_3(\text{Cu}_{0.6}\text{Ge}_{0.4})\text{N}$ displays NTE behavior around room temperature (295–245 K). However, with increasing the amount of Si from 0.05 to 0.2, the NTE temperature moves constantly toward lower temperature region. For example, the NTE in $\text{Mn}_3(\text{Cu}_{0.6}\text{Si}_{0.05}\text{Ge}_{0.35})\text{N}$ occurs in the temperature range of 210–270 K, while for $\text{Mn}_3(\text{Cu}_{0.6}\text{Si}_{0.1}\text{Ge}_{0.3})\text{N}$ and $\text{Mn}_3(\text{Cu}_{0.6}\text{Si}_{0.15}\text{Ge}_{0.25})\text{N}$ the NTE takes place from 170 to 238 K and from 90 to 190 K, respectively. This fact indicates the significant effect of partial substitution of Si for Ge and as well confirms our expectation.

Furthermore, another important feature to be stressed is that the volume change in NTE becomes gradual and the corresponding operation-temperature window becomes broader with increasing Si content. Typically, the NTE operation-temperature window of $\text{Mn}_3(\text{Cu}_{0.6}\text{Si}_{0.05}\text{Ge}_{0.35})\text{N}$ and $\text{Mn}_3(\text{Cu}_{0.6}\text{Si}_{0.1}\text{Ge}_{0.3})\text{N}$ are 60 and 68 K, respectively, whereas for $\text{Mn}_3(\text{Cu}_{0.6}\text{Si}_{0.15}\text{Ge}_{0.25})\text{N}$ the NTE operation-temperature window reaches a value of 100 K, which is almost twice larger than that of $\text{Mn}_3(\text{Cu}_{0.6}\text{Ge}_{0.4})\text{N}$. On the other hand, it should be noted that $\text{Mn}_3(\text{Cu}_{1-x}\text{Ge}_x)\text{N}$ also displays NTE behavior at low temperatures when reducing the amount of Ge, as Takenaka and Takagi reported.⁹ For a comparison, we prepared samples $\text{Mn}_3(\text{Cu}_{0.7}\text{Ge}_{0.3})\text{N}$ and $\text{Mn}_3(\text{Cu}_{0.8}\text{Ge}_{0.2})\text{N}$, and compared their linear thermal expansion data with the data for $\text{Mn}_3(\text{Cu}_{0.6}\text{Si}_{0.15}\text{Ge}_{0.25})\text{N}$, as shown in Fig. 2(b). We find that the volume change in NTE is very sharp and discontinuous and the NTE operation-temperature window is very narrow in $\text{Mn}_3(\text{Cu}_{0.7}\text{Ge}_{0.3})\text{N}$ and

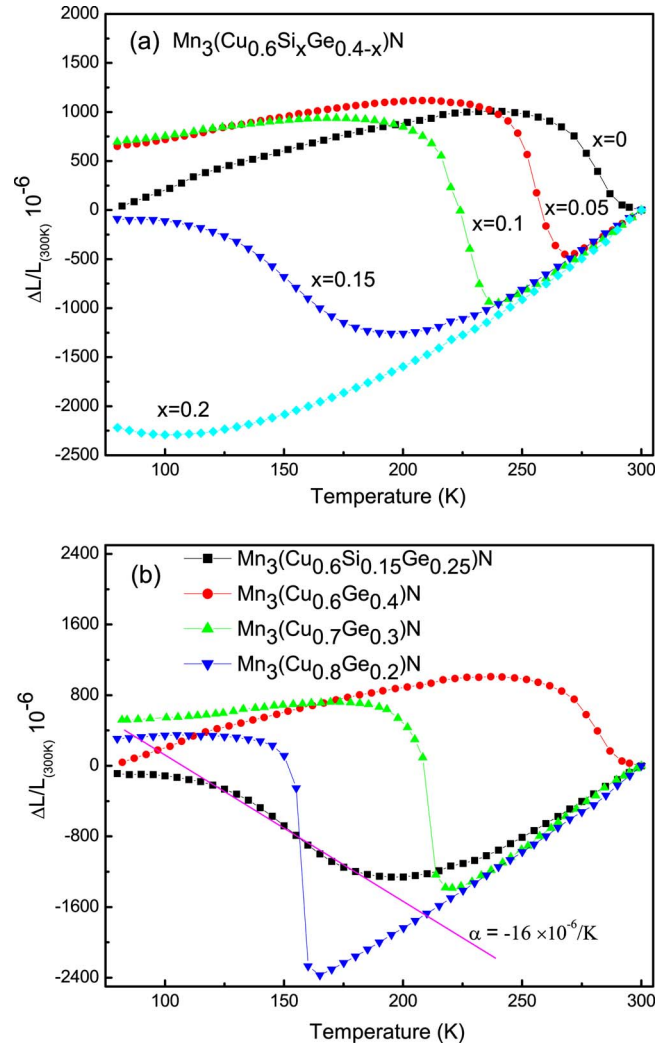


FIG. 2. (Color online) Linear thermal expansion of (a) $\text{Mn}_3(\text{Cu}_{0.6}\text{Si}_x\text{Ge}_{0.4-x})\text{N}$ ($x=0, 0.05, 0.1, 0.15, 0.2$) and (b) $\text{Mn}_3(\text{Cu}_{0.6}\text{Si}_{0.15}\text{Ge}_{0.25})\text{N}$, $\text{Mn}_3(\text{Cu}_{0.6}\text{Ge}_{0.4})\text{N}$, $\text{Mn}_3(\text{Cu}_{0.7}\text{Ge}_{0.3})\text{N}$, and $\text{Mn}_3(\text{Cu}_{0.8}\text{Ge}_{0.2})\text{N}$.

$\text{Mn}_3(\text{Cu}_{0.8}\text{Ge}_{0.2})\text{N}$, while for $\text{Mn}_3(\text{Cu}_{0.6}\text{Si}_{0.15}\text{Ge}_{0.25})\text{N}$, the NTE operation-temperature window is much broadened. This comparison clearly demonstrates the advantage of the $\text{Mn}_3(\text{Cu}_{1-x}\text{Ge}_x)\text{N}$ with Si doping over that without Si doping in terms of ΔT at low temperatures. Furthermore, for $\text{Mn}_3(\text{Cu}_{0.6}\text{Si}_{0.15}\text{Ge}_{0.25})\text{N}$, we obtained an average thermal expansion coefficient of $\alpha = -16 \times 10^{-6} \text{ K}^{-1}$ in the temperature range of 120–184 K, in which the thermal expansion data are nearly linear. The absolute magnitude of this NTE is comparable to its positive counterpart seen in most common metals such as copper, the thermal expansion coefficients of which are and $15.57 \times 10^{-6} \text{ K}^{-1}$ at 210 K.¹³

NTE in manganese nitrides Mn_3AN has been reported to be due to the MVE accompanied by the change in magnetic ordering.¹⁴ Here, we measured the magnetic properties of the studied compounds, although the detailed magnetic structure has yet to be examined. Figure 3(a) shows the temperature dependence of the inverse magnetic susceptibility for all the samples. At enough high temperatures, the samples show typical paramagnetic behavior. When decreasing the temperature, magnetic transitions take place. For example, $\text{Mn}_3(\text{Cu}_{0.6}\text{Si}_x\text{Ge}_{0.4-x})\text{N}$ ($x=0.05, 0.1$) exhibit a paramagnetic to antiferromagnetic transition at 270 and 230 K, respec-

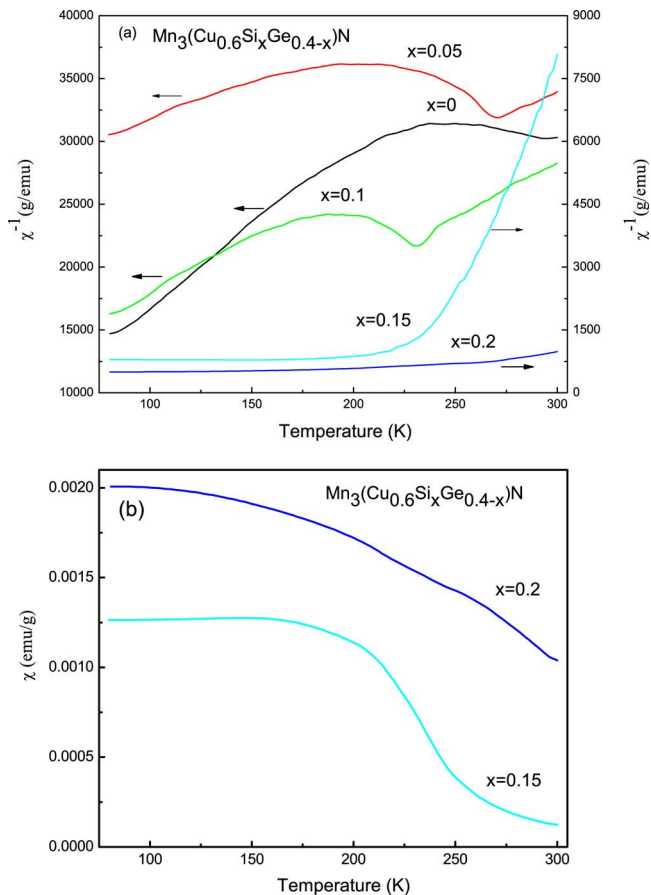


FIG. 3. (Color online) Temperature dependence of (a) the reciprocal magnetic susceptibility of $\text{Mn}_3(\text{Cu}_{0.6}\text{Si}_x\text{Ge}_{0.4-x})\text{N}$ ($x=0, 0.05, 0.1, 0.15, 0.2$), and (b) the magnetic susceptibility of $\text{Mn}_3(\text{Cu}_{0.6}\text{Si}_x\text{Ge}_{0.4-x})\text{N}$ ($x=0.15, 0.2$).

tively. This magnetic transition is accompanied by the NTE, which is quite similar to that demonstrated in Ref. 9.

For $\text{Mn}_3(\text{Cu}_{0.6}\text{Si}_x\text{Ge}_{0.4-x})\text{N}$ ($x=0.15, 0.2$), however, an obviously different magnetic transition occurs [Fig. 3(a)]. The magnetic susceptibility increases gradually with decreasing temperature in a wide temperature range [Fig. 3(b)]. This gradual change in magnetic ordering is typical of a paramagnetic to spin-canted ferromagnetic transition, and it is concurrent with a large, continuous NTE [Fig. 2(a)]. We should note that such a correspondence of this type of magnetic transition to NTE observed here is consistent with the result obtained in $\text{La}(\text{Fe}_x\text{Si}_{1-x})_{13}$,¹⁵ although it is exceptionally different from the observations obtained in $\text{Mn}_3(\text{Cu}_{1-x}\text{Ge}_x)\text{N}$, in which a gradual change of NTE is accompanied by a paramagnetic to antiferromagnetic transition.⁹

Partial substitution of Ge by Si in $\text{Mn}_3(\text{Cu}_{0.6}\text{Ge}_{0.4})\text{N}$ has now been demonstrated to shift the transition temperature of NTE obviously to a lower temperature region. This result consists of the MVE identified in Mn_3AN . The magnetic transition temperature of Mn_3AN is scaled by electron concentration around element A.⁸ Si and Ge are both in group 4B in the periodic table, with Si lying above Ge, i.e., they have four valence electrons but Si has one subshell fewer than Ge. It is noted that the tendency for an atom to lose its

electrons decreases as the size of the atom shrinks, due to its relative ability to hold on to its outer electrons. This means that Si doping, when compared to Ge doping, has fewer free electrons in Mn_3AN at a given temperature and accordingly, the electron concentration will be decreased when Si partially substitutes for Ge. As a result, the transition temperature of magnetic ordering and as well NTE shifts toward lower temperature region with increasing Si content.

The obvious broadening of the NTE operation-temperature window in $\text{Mn}_3(\text{Cu}_{0.6}\text{Ge}_{0.4})\text{N}$ with increasing amount of Si is associated with the MVE as well, which is dominated by the Mn–Mn interaction in the manganese nitride. As pointed out by Iikubo *et al.*,¹⁶ the exchange interactions between the nearest-neighbor Mn moments give rise to geometrical frustration and large MVE in $\text{Mn}_3(\text{Cu}_{1-x}\text{Ge}_x)\text{N}$. In our case, the exchange interactions between the nearest-neighbor Mn moments are presumed to be further disturbed in the presence of Si. Thus, the spin canting may appear in samples $\text{Mn}_3(\text{Cu}_{0.6}\text{Si}_x\text{Ge}_{0.4-x})\text{N}$ ($x=0.15, 0.2$), which might give rise to a relaxorlike behavior and accordingly might broaden the NTE operation-temperature window.

In conclusion, we have successfully synthesized the $\text{Mn}_3(\text{Cu}_{0.6}\text{Si}_x\text{Ge}_{0.4-x})\text{N}$ with excellent NTE behavior at cryogenic temperatures. The NTE temperature shifts toward low-temperature region and the NTE operation-temperature window becomes broader with increasing the amount of Si dopants. Typically, a large NTE coefficient of $-16 \times 10^{-6} \text{ K}^{-1}$ and a broad NTE operation-temperature window of 100 K were obtained in the $\text{Mn}_3(\text{Cu}_{0.6}\text{Si}_{0.15}\text{Ge}_{0.25})\text{N}$. Consequently, we believe that the studied manganese nitride Mn_3CuN codoped with Ge and Si has the potential for cryogenic applications.

This work was supported by the Chinese National Foundation of Natural Science Research (Grant No. 50676101) and the CAS Chinese Oversea Outstanding Scholar Foundation (No. 2006-1-17).

¹J. S. O. Evans, Z. Hu, J. D. Jorgensen, D. N. Argyriou, S. Short, and A. W. Sleight, *Science* **275**, 61 (1997).

²Y. M. Hao, Y. Gao, B. W. Wang, J. P. Qu, Y. X. Li, J. F. Hu, and J. C. Deng, *Appl. Phys. Lett.* **78**, 3277 (2001).

³C. A. Perottoni and J. A. H. da Jornada, *Science* **886**, 280 (1998).

⁴T. A. Mary, J. S. O. Evans, T. Vogt, and A. W. Sleight, *Science* **272**, 90 (1996).

⁵J. S. O. Evans, T. A. Mary, T. Vogt, M. A. Subramanian, and A. W. Sleight, *Chem. Mater.* **8**, 2809 (1996).

⁶K. Lagarec and D. G. Rancourt, *Phys. Rev. B* **62**, 978 (2000).

⁷G. Hausch, R. Bächer, and J. Hartmann, *Physica B (Amsterdam)* **161**, 22 (1989).

⁸D. Fruchart and E. Bertaut, *J. Phys. Soc. Jpn.* **44**, 781 (1978).

⁹K. Takenaka and H. Takagi, *Appl. Phys. Lett.* **87**, 261902 (2005).

¹⁰K. Takenaka, K. Asano, M. Misawa, and H. Takagi, *Appl. Phys. Lett.* **92**, 011927 (2008).

¹¹R. K. Kirby and T. A. Hahn, Certificate of Analysis, 1971.

¹²JCPDS Card No. 23-0220.

¹³R. K. Kirby and T. A. Hahn, National Bureau of Standards Certificate, 1975.

¹⁴T. Moriya and K. Usami, *Solid State Commun.* **34**, 95 (1980).

¹⁵A. Fujita, S. Fujieda, and K. Fukamichi, *Phys. Rev. B* **65**, 014410 (2001).

¹⁶S. Iikubo, K. Kodama, K. Takenaka, H. Takagi, and S. Shamoto, *Phys. Rev. B* **77**, 020409 (2008).